Collision-induced dissociation and photodetachment of singly and doubly charged anionic polynuclear transition metal carbonyl clusters: $Ru_3Co(CO)_{13}^-$, $Ru_6C(CO)_{16}^{2-}$, and $Ru_6(CO)_{18}^{2-}$

Colin P. G. Butcher, Brian F. G. Johnson, and J. Scott McIndoe
Department of Chemistry, The University of Cambridge, Lensfield Road, Cambridge CB2 1EW, United Kingdom

Xin Yang, Xue-Bin Wang, and Lai-Sheng Wang[a)]
Department of Physics, Washington State University, Richland, Washington 99352 and W. R. Wiley Environmental Molecular Sciences Laboratory, Pacific Northwest National Laboratory, MS K8-88, Richland, Washington 99352

Three polynuclear transition metal carbonyl cluster anions, $Ru_3Co(CO)_{13}^-$, $Ru_6C(CO)_{16}^{2-}$, and $Ru_6(CO)_{18}^{2-}$ have been studied using energy-dependent electrospray ionization mass spectrometry (EDESI–MS) and photodetachment photoelectron spectroscopy (PES). EDESI–MS maps show a simple collision-induced dissociation (CID) process for $Ru_3Co(CO)_n^-$ by stripping CO down to the metal core. For the doubly charged species, two competing CID channels were observed, viz. loss of neutral CO and loss of $CO + e^-$. It was found that the parent dianions first lose neutral CO down to $n=9$, producing a series of dianions, $Ru_6C(CO)_n^{2-}$ ($n=9-16$) and $Ru_6(CO)_n^{2-}$ ($n=9-18$). For $n<9$, the dianions become electronically unstable against autodetachment, and singly charged anions, $Ru_6C(CO)_n^-$ and $Ru_6(CO)_n^-$ ($n=0-9$), were observed. The PES spectra of the dianions show the electron binding energies decrease monotonically as n decreases and become ~ 0.0 eV for $n=9$, in exact agreement with the CID patterns that reflect the electronic instability of the doubly charged metal complexes with $n<9$. All of the PES spectra show congested features, indicating very high density of low-lying electronic states for the transition metal carbonyl clusters. The electron binding energies of $Ru_3Co(CO)_n^-$ are similar for $n=4-13$, but decrease sharply from $n=4$ to 0. The intramolecular Coulomb repulsion in the dianions was observed to increase with loss of CO, ranging from ~ 1.8 eV for $Ru_6C(CO)_{16}^{2-}$ to ~ 2.4 eV for $Ru_6C(CO)_9^{2-}$. © *2002 American Institute of Physics.* [DOI: 10.1063/1.1462579]

I. INTRODUCTION

Transition metal carbonyl complexes have played major roles in modern inorganic chemistry.[1] They are important in coordination chemistry and organometallic chemistry and have been used in many chemical processes such as catalysis.[2] Carbonyl complexes are often considered as models for CO binding to a metal surface.[3] The metal-CO bonding involves σ donation from the filled CO 5σ orbital to the metal and the π back bonding from the metal $d\pi$ orbitals to the unfilled carbonyl $p\pi^*$ orbitals.[4] There have been extensive theoretical and experimental studies on the transition metal carbonyl complexes.[5–13] Most of these studies have been focused on the mononuclear carbonyl complexes with a few on the dinuclear complexes. Polynuclear transition metal carbonyl clusters are more important models for CO binding to metal surfaces and they also exhibit interesting redox chemistries. However, relatively little is known about the dissociation energies of the carbonyl ligands and excess electron binding energies of the anionic polynuclear species, which are crucial in understanding the chemical bonding, electronic structures, and thermal chemistries of these clusters.

Energy-dependent electrospray ionization mass spectrometry (EDESI–MS) has been used to present the complete fragmentation patterns of transition metal carbonyl cluster monoanions.[14] Collision-induced dissociation (CID) either at the skimmer cone[15] or in the collision cell (for EDESI–MS/MS)[16] results in stripping of the ligands from the cluster, generally down to the metal core. The data are depicted in a compact map format and essentially summarize the fragmentation information contained in hundreds of individual spectra collected at different collision energies. Photodetachment photoelectron spectroscopy (PES) is a powerful technique to investigate the electronic structure of a variety of cluster species, directly yielding the excess electron binding energies of the clusters. A number of singly charged anionic transition metal carbonyls have been studied by PES.[10] We have developed a PES apparatus coupled with an electrospray ion source, specifically designed to investigate gaseous multiply charged anions (MCAs) as well as singly charged anions from solutions.[17,18] As shown previously,[19,20] this technique is well suited to probe both multiply and singly charged metal complex anions, providing unprecedented details of molecular electronic structure information and excess electron binding energies. In addition, the stability of MCAs with respect to electron detachment and charge-separation fragmentation has been investigated.[21,22]

a)Electronic mail: ls.wang@pnl.gov

       6560

J. Chem. Phys., Vol. 116, No. 15, 15 April 2002

Photodetachment of transition metal clusters   6561

In the current paper, we report a combined EDESI–MS and PES study of three anionic polynuclear transition metal carbonyl clusters, $Ru_3Co(CO)_n^-$, $Ru_6C(CO)_n^{2-}$, and $Ru_6(CO)_n^{2-}$. Several issues were addressed in this investigation: (1) to obtain the electron binding energies of the clusters and their change as a function of CO number, n; (2) to understand the fragmentation pattern of the clusters, particularly, via two competing channels of CO loss and $CO + e$ loss for the dianionic clusters; (3) to search for the smallest stable doubly charged cluster anions. By combining these two experimental methods, we show that a complete pattern of dissociation of the ligands and the electronic stability of the anionic clusters can be readily revealed.

II. EXPERIMENTAL METHODS

Three carbonyl compounds, $[PPN][Ru_3Co(CO)_{13}]$,[23] $[PPN]_2[Ru_6C(CO)_{16}]$,[24] and $[PPN]_2[Ru_6(CO)_{18}]$[25] [PPN = bis(triphenylphosphino)iminium cation], were prepared according to literature procedures. All reactions were carried out under a nitrogen atmosphere.

A. Mass spectrometry instrumentation

EDESI and ESI mass spectra were collected using a Micromass Quattro LC instrument in negative-ion mode, with CH_2Cl_2 as the mobile phase. The nebulizer tip was at 3.1 kV and 90 °C, and N_2 was used as the bath gas. Samples were introduced directly to the source at 2–4 μL/min via a syringe pump. The cone voltage was ramped from 0 to 200 V for the EDESI–MS spectra, and the collision voltage was ramped from 0 to 200 V for the EDESI–MS/MS spectra. Contours on the maps correspond to evenly spaced increments between upper and lower limits selected to maximize the number of fragments apparent in the map (upper limit) while eliminating noise (lower limit). The mass spectrum across the top of the map represents a summation of all spectra used to generate the map and is therefore the best indicator of the relative intensity of each of the fragment ions. Resolution settings are kept low to enhance the signal-to-noise ratio.

B. Photodetachment photoelectron spectroscopy

The PES experiments were performed with a magnetic-bottle time-of-flight (TOF) PES apparatus coupled with a home-built electrospray source. Details of the apparatus have been published elsewhere[17] and only a brief description is given here. A 10^{-4} M solution of each sample in an acetonitrile solvent was sprayed through a 0.01 mm diameter syringe needle (biased at -2.2 kV) under N_2 atmosphere. The resulting charged droplets were fed into a desolvation capillary heated to ∼50 °C. The desolvation capillary was biased by a negative DC voltage relative to the skimmer along the sampling path to achieve CID. The voltage was typically ramped from 0 to -350 V for the whole range of CID products from the parent to the most fragmented clusters. Anions formed in the desolvation capillary and the CID products were guided by a radio-frequency quadrupole device into a quadrupole ion trap. Ions were accumulated for 0.1 second in the trap before being pulsed out into the extraction zone of a TOF mass spectrometer. The dominant anion signals in each
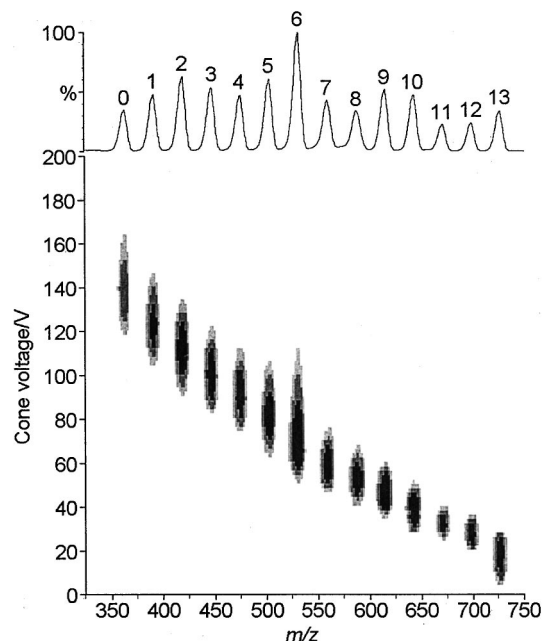

FIG. 1. EDESI–MS negative-ion mass spectrum of $Ru_3Co(CO)_{13}^-$.

case were the parent anions and their CID fragments; both dianions and monoanions. The anions of interest were mass-selected and decelerated before being intercepted by a probe laser beam in the detachment zone of the magnetic-bottle electron analyzer. Both a Nd:YAG laser (266 nm) and an excimer laser (193 and 157 nm) were used for photodetachment in the current experiment. Photoelectrons were collected at nearly 100% efficiency by the magnetic-bottle and analyzed in a 4 m long electron flight tube. Photoelectron TOF spectra were collected and then converted to kinetic energy spectra, calibrated by the known spectra of I^- and O^-. The electron binding energy spectra were obtained by subtracting the kinetic energy spectra from the detachment photon energies. The electron kinetic energy resolution was ∼2% ($\Delta E/E$), i.e., 20 meV for 1 eV electrons.

III. RESULTS

A. EDESI–MS spectra

1. Monoanionic species

The EDESI–MS map of the monoanion $Ru_3Co(CO)_{13}^-$ shows a straightforward pattern of CO loss as the cone voltage is increased (Fig. 1). Each of the cross peaks in the map depicts one of the ions, $Ru_3Co(CO)_n^-$ ($n = 0$–13). At the lowest cone voltages (0–20 V), only the parent ion $Ru_3Co(CO)_{13}^-$ can be observed, but by 40 V this ion is no longer present in the mass spectrum and $Ru_3Co(CO)_n^-$ ($n = 9$–12) have appeared. This pattern continues consistently until the appearance of the bare metal core (Ru_3Co^-) at 120 V, which survives until 165 V. The $Ru_3Co(CO)_6^-$ cluster seemed to show some extra stability relative to its neighbors. It has been shown that the ligands of tetranuclear clusters can be stripped off at an appreciably lower energy than that of hexanuclear clusters. For example, the clusters, $Rh_6(CO)_{15}(COOMe)^-$, $Rh_6(CO)_{16}(COOMe)^-$, $Ru_5CoC(CO)_{16}^-$ and $HRu_4Co_2C(CO)_{15}^-$, require voltages of ∼180 V
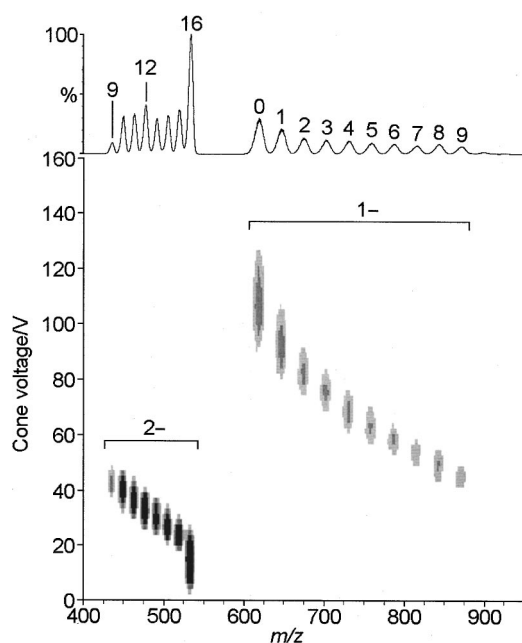
FIG. 2. EDESI–MS negative-ion mass spectrum of $Ru_6C(CO)_{16}^{2-}$.

FIG. 3. Photoelectron spectra of $Ru_3Co(CO)_n^-$ ($n=0-13$) at 193 nm (6.424 eV).

to generate the cluster cores,[14] compared to 120 V for $Ru_3Co(CO)_{13}^-$ and 100 V for $RuCo_3(CO)_{12}^-$. Some of these variations may be due to the relative bond energies, but the main feature is probably simply the mass-to-charge ratio of the parent ions. Those clusters with low mass-to-charge ratios are accelerated faster in the skimmer cone region (pressure of ~1 Torr, so a multicollision region) and therefore have more energetic collisions with the residual bath gas. More sluggish collisions occur with the heavier clusters and therefore a higher cone voltage is required to strip them down to the metal cores.

2. Dianionic species

A consistent difference in fragmentation behavior was observed in the EDESI–MS maps of the dianionic species. For $Ru_6C(CO)_{16}^{2-}$ (Fig. 2), the map shows that at low cone voltages (0–20 V) only the parent dianion is present at 533 m/z. At 20 V, a new peak appears 14 m/z lower, corresponding to $Ru_6C(CO)_{15}^{2-}$ due to the loss of a neutral CO. The CO loss continues with increasing cone voltage until ~50 V, at which point a competition between the formation of the dianionic $Ru_6C(CO)_9^{2-}$ at 435 m/z and its monoanion $Ru_6C(CO)_9^-$ at 870 m/z occurred. The loss of an electron may occur before, concomitant with, or after the CO loss. But it was clear CO^- loss did not happen because this species was not observed in the MS/MS spectrum and CO is also known not to bind an extra electron. With increasing cone voltage, a series of CO losses from the monoanion $Ru_6C(CO)_9^-$ took place down to the carbon-centered cluster core Ru_6C^- at 618 m/z. The generation of the completely CO-stripped cluster core occurred at ~100 V, a very low cone voltage for a parent complex as large as $Ru_6C(CO)_{16}^{2-}$ with a molecular weight of 1066 Da. This observation suggests that the loss of the electron occurred after the CID processes, but before the ion was transferred to the mass analyzer. Further inspection of the map revealed that except
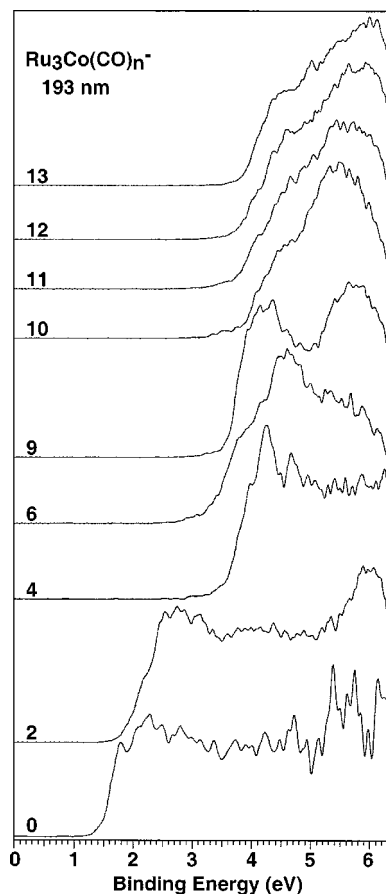
for the most decarbonylated monoanions ($n=0$ and 1) all the other monoanions have relatively short lifetimes and weak intensities, as revealed by the narrow cone voltage ranges.

The EDESI–MS map for $Ru_6(CO)_{18}^{2-}$ (not shown) is very similar to that of $Ru_6C(CO)_{16}^{2-}$. Again, just the parent dianion was present at low cone voltages with the onset of CO loss at ~8 V, significantly lower than that for the carbide-centered complex. Successive loss of eight CO ligands occurred to $Ru_6(CO)_{10}^{2-}$, at which point both loss of CO to form $Ru_6(CO)_9^{2-}$ and loss of an electron to form the monoanion $Ru_6(CO)_{10}^{2-}$ at 886 m/z took place. A series of peaks, 28 m/z apart, appeared with increasing cone voltages, corresponding to stripping of the CO ligands from the monoanions down to the Ru_6^- cluster core at 606 m/z.

B. Photoelectron spectra

The PES spectra of the three cluster series, $Ru_3Co(CO)_n^-$ ($n=0-13$), $Ru_6C(CO)_n^{2-}$ ($n=9-16$), and $Ru_6(CO)_n^{2-}$ ($n=9-18$), are shown in Figs. 3–5, respectively. The monoanion mass signals from the CID products for $Ru_6C(CO)_n^-$ ($n=0-9$), and $Ru_6(CO)_n^-$ ($n=0-9$) were too weak and their PES spectra were not able to be measured.
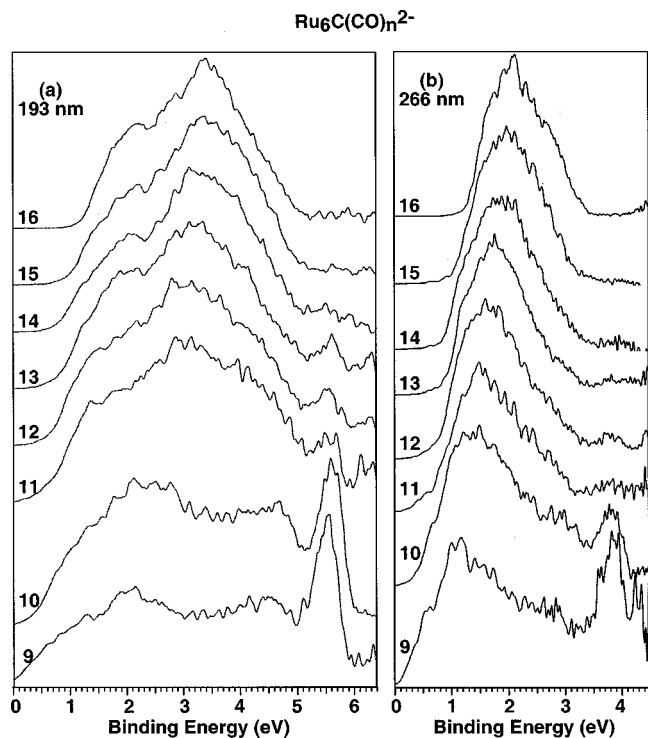
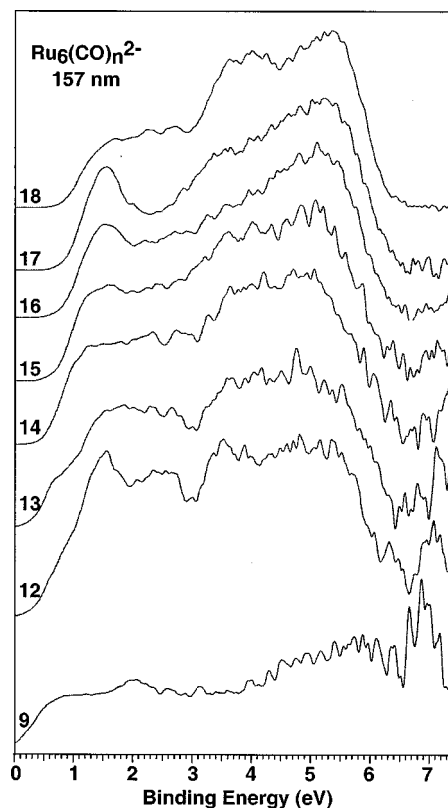FIG. 4. Photoelectron spectra of $Ru_6C(CO)_n^{2-}$ ($n=9-16$) at (a) 193 nm and (b) 266 nm (4.661 eV).

FIG. 5. Photoelectron spectra of $Ru_6(CO)_n^{2-}$ ($n=9-18$) at 157 nm (7.866 eV).

1. $Ru_3Co(CO)_n^-$

Figure 3 shows the PES spectra of $Ru_3Co(CO)_n^-$ ($n=0-13$), measured at 193 nm. The spectra of several species ($n=1, 3, 5, 7, 8$) are missing due to overlaps with other CID mass signals under our experimental conditions. We also obtained the spectra of Ru_3Co^- and $Ru_3Co(CO)_2^-$ (not shown) at 266 nm and resolved a sharp threshold feature in each case, which appeared as shoulders in the 193 nm spectra (Fig. 3). Other members of the $Ru_3Co(CO)_n^-$ series have too high electron binding energies and were not investigated at 266 nm. All the spectra were broad, suggesting high density of low-lying electronic states for all the $Ru_3Co(CO)_n$ neutral clusters. The adiabatic electron detachment energies (ADEs), i.e., the electron affinities of the corresponding neutral $Ru_3Co(CO)_n$ were determined by drawing a straight line along the low binding energy side of the PES spectra and then adding the instrumental resolution to the intersection to the binding energy axis. This procedure, though approxi-

mate, yielded consistent ADE values for PES spectra with sharp thresholds. The estimated ADEs are given in Table I and shown in Fig. 6(a). It is seen that the ADEs from the $Ru_3Co(CO)_n^-$ cluster with $n=13-4$ are roughly constant but then decrease sharply from $n=4$ to 0.

2. $Ru_6C(CO)_n^{2-}$

The PES spectra of $Ru_6C(CO)_n^{2-}$ ($n=9-16$) are shown in Fig. 4 at two photon energies. The doubly charged clusters with $n<9$ were not observed under our experimental conditions, consistent with the EDESI–MS spectra (Fig. 2). All the spectra are highly congested with no resolution of fine structures, even at 266 nm. The ADEs, measured from the thresholds of the PES spectra, are given in Table I and shown in Fig. 6(b). It is observed that the ADEs gradually decrease with loss of the CO ligands and approach to almost 0 eV at

TABLE I. Adiabatic electron binding energies of $Ru_3Co(CO)_n^-$, $Ru_6C(CO)_n^{2-}$, and $Ru_6(CO)_n^{2-}$ in eV.[a]

				$Ru_3Co(CO)_n^-$					
n	13	12	11	10	9	6	4	2	0
	3.90	3.83	3.77	3.88	3.68	3.36	3.63	1.95	1.55
					$Ru_6C(CO)_n^{2-}$				
n	16	15	14	13	12	11	10	9	
	1.30	1.05	0.85	0.85	0.74	0.62	0.39	0.08	
					$Ru_6(CO)_n^{2-}$				
n	18	17	16	15	14	13	12	9	
	0.95	0.95	0.90	0.79	0.62	0.39	0.37	0.00	

[a]Accuracy ± 0.10 eV.
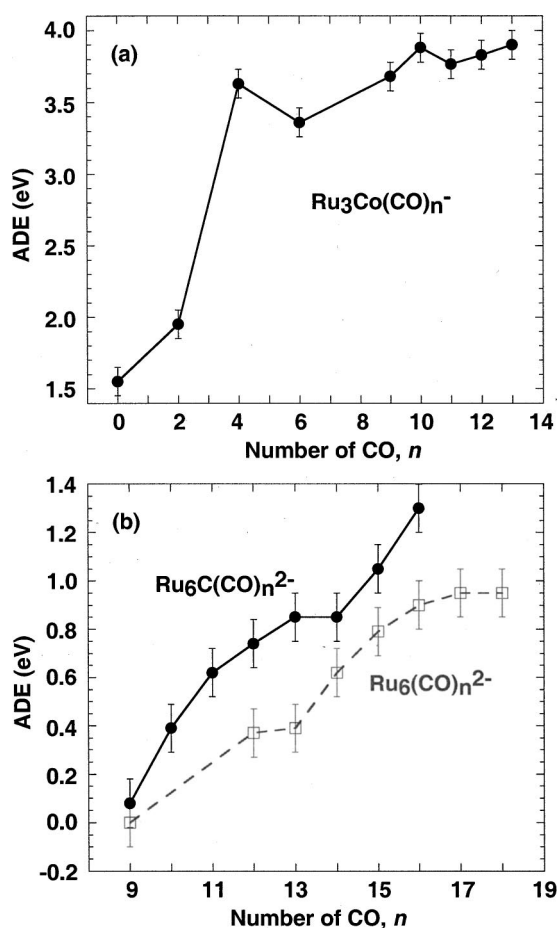
FIG. 6. Adiabatic electron binding energies of (a) $Ru_3Co(CO)_n^-$ and (b) $Ru_6C(CO)_n^{2-}$ (solid circles) and $Ru_6(CO)_n^{2-}$ (open squares) as a function of the number of CO ligands, n.

$n=9$. These results are in exact agreement with the mass spectral pattern, in which no dianions for $n<9$ were observed due to their electronic instability against electron autodetachment.

Each spectrum in Fig. 4 appeared to be cut off at the high binding energy side (the sharp high binding energy peak in the spectra of $n=9$ and 10 will be discussed below). The cutoff was more visible in the 193 nm spectra for $n=14-16$ beyond 5.0 eV [Fig. 4(a)] and in the 266 nm for $n=12-16$ beyond 3.0 eV. This cutoff was due to a repulsive Coulomb barrier (RCB), which exists universally in MCAs due to the intramolecular Coulomb repulsion and prevents slow electrons from being emitted.[18] The RCB effects on the PES data were seen most clearly in the 266 nm relative to the 193 nm spectra, where spectral features were seen up to ~5 eV, but were severely cutoff in the 266 nm spectra. On the basis of the spectral cutoff, the magnitude of the RCB could be estimated by subtracting the binding energies at the cutoff point from the photon energies. Using this approximate procedure for the data sets at both photon energies, we estimated the RCB of $Ru_6C(CO)_n^{2-}$ to gradually increase from ~1.8 eV ($n=16$) to ~2.4 eV ($n=9$). The RCB is equivalent to the intramolecular Coulomb repulsion, which is expected to increase for decreasing cluster size. Our estimated RCB is

consistent with the trend of the ADEs and the trend of the cluster size.

The sharp and intense peaks at the high binding energy side in the spectra of $n=9$ and 10 were surprising, because they seemed to occur in the cutoff regime as discussed above. Several observations were made for this sharp peak. First, it existed only for the most decarbonylated clusters. Second, it was observed in the PES spectra of the same species at all detachment photon energies, 266, 193, and 157 nm (not shown), and the kinetic energies of the emitted electrons corresponding to this peak were roughly the same at the different photon energies. Third, the relative intensity of this peak increased in the spectra at higher photon energies, as shown in Fig. 4. Finally, the intensity of this peak was linearly proportional to the photon flux. The origin of this peak will be discussed later.

3. $Ru_6(CO)_n^{2-}$

The PES spectra for $Ru_6(CO)_n^{2-}$ ($n=9-18$) were only taken at 157 nm and are shown in Fig. 5. The spectra are all very broad and congested. The ADEs were observed to gradually decrease with loss of CO, reaching to ~0 eV for $n=9$. Similar to the $Ru_6C(CO)_n^{2-}$ system, this observation is consistent with the mass spectral pattern, where no dianions were detected for $n<9$. The ADEs of $Ru_6(CO)_n^{2-}$ are given in Table I. They are consistently smaller than those of $Ru_6C(CO)_n^{2-}$, as shown in Fig. 6(b). Spectral cutoff at the high binding energy side was also observed due to the RCB, similar to the spectra of $Ru_6C(CO)_n^{2-}$. Again, a relative sharp feature at ~6.9 eV was observed in the spectra of the most decarbonylated species, discernible starting from $n=12$. This peak was reproducible and was similar to the sharp peaks observed for the smaller $Ru_6C(CO)_n^{2-}$ systems (Fig. 4).

IV. DISCUSSIONS

A. Stability of the doubly charged cluster complexes in the gas phase

MCAs are ubiquitous in nature and are important chemical species in solutions and solids. However, free MCAs have been difficult to study and very few of them have been known until very recently.[18,26] The strong intramolecular Coulomb repulsion between the excess charges tends to make these species rather unstable in the gas phase. Indeed, this is the reason why most of the common inorganic dianions, such as SO_4^{2-} or CO_3^{2-}, would spontaneously emit one electron when they are brought into the gas phase without the stabilizing effects of counter ions or solvent molecules.[27–29] As shown in Figs. 4–6, the ADEs of $Ru_6C(CO)_n^{2-}$ and $Ru_6(CO)_n^{2-}$ decrease monotonically with the loss of CO, and approach 0 eV at $n=9$. From the trend of the ADEs shown in Fig. 6(b), we can extrapolate that ADEs of the smaller clusters ($n<9$) for both cluster series would be negative, and hence electronically unstable in the gas phase. This observation is in exact agreement with the EDESI–MS results (Fig. 2), which showed that for $n<9$ only singly charged complexes were observed. The fact that no singly charged anions $Ru_6C(CO)_n^-$ and $Ru_6(CO)_n^-$ for n

>9 were observed in EDESI–MS suggested that ligand loss during CID was the only process and there was no electron loss due to CID, even for those doubly charged anions that have very low ADEs. Therefore, all the monoanions were likely formed from electron loss following CO losses. However, as we mentioned earlier, MCAs all possess a RCB, which gives them dynamic stability, i.e., finite lifetimes. That none of the dianions with $n<9$ was observed was probably due to the current CID conditions and did not reflect the intrinsic lifetimes of these MCAs.

B. Electron binding energies of the clusters

The CO ligands in $Ru_6C(CO)_n^{2-}$ and $Ru_6(CO)_n^{2-}$ are bound to the central octahedral cluster cores $[Ru_6C]$ and $[Ru_6]$ via metal–carbon bonding.[24,25] The physical dimensions of the clusters from the parent ions down to the $n=9$ fragments remain approximately the same, despite the decrease in the number of CO ligands. The excess charge in the dianion is expected to be mainly localized on the central cluster core. The electronic stability of the dianion is then largely determined by the cluster–ligand interactions. Because carbon and oxygen are more electronegative than ruthenium, the CO ligands are expected to withdraw charge from the cluster core through $d-\pi^*$ back donation, thereby reducing the Coulomb repulsion and increasing the electron binding energies. A recent theoretical study of the transition metal–carbonyl bond in mononuclear hexacarbonyl anionic complexes confirm that indeed the CO ligands have more negative charge density than the metal.[8] Thus, the loss of CO results in the distribution of the negative charges amongst the remaining fewer ligands and the metal core, increasing the intramolecular Coulomb repulsion and reducing the electron binding energy. The consistently smaller ADEs of $Ru_6(CO)_n^{2-}$ compared to those of $Ru_6C(CO)_n^{2-}$ arise from the central electronegative carbon atom, which helps stabilize the negative charges and also makes the Ru_6C cluster core larger, further reducing the electron–electron Coulomb repulsion. As shown in Fig. 6(b), the ADEs for both the cluster series show a nonlinear dependence on the ligand number, likely due to the different symmetries of the complexes, which in turn influence the detailed cluster–ligand bonding.

Figure 6(a) shows the electron binding energies of $Ru_3Co(CO)_n^-$ as a function of ligand number. The ADEs remain almost unchanged from $n=13$ to 4 and then sharply decrease from 4 to 0. The Ru_3Co cluster core has a distorted tetrahedral structure.[23] With $n>4$, each metal site is bound to at least one carbonyl ligand, and the excess electron binding energy is not sensitive to further CO binding. However, from $n=4$ to 0, the number of totally naked metal binding sites increases, leading to the sharp decrease of electron binding energies in agreement with the low electron binding energy of the bare metal core.

C. Interpretation of the PES spectra

The PES spectra of $Ru_3Co(CO)_n^-$, $Ru_6C(CO)_n^{2-}$, and $Ru_6(CO)_n^{2-}$ show very broad and congested features, even for the smallest Ru_3Co^- cluster. The diffuse spectra could be due to two sources, dense low-lying electronic states and internally hot clusters. Vibrationally hot clusters yield broad PES spectra as a result of hot band transitions. Our electrospray source was operated at room temperature. However, except for the parent anions, all the daughter anions were produced by CID, which could result in very hot clusters. In order to test the temperature effects, we produced Ru_3Co^- cluster using a laser vaporization cluster source,[30] where we can control and vary the cluster temperatures to a limited degree.[31] As we showed previously with Al cluster anions,[32] we can produce "cold" clusters in the laser vaporization source around or slightly below room temperature, "warm" clusters around 500–800 K, and hot clusters as high as 1000 K. We did find a slight temperature dependence of the Ru_3Co^- PES spectrum[30] and found that the spectrum from the CID product corresponded to at least the "warm" conditions of the laser vaporization-produced clusters. However, even the spectrum taken at the "cold" condition still showed a similar continuous band structure.[30] Therefore, the congested spectra in Figs. 3–5 were basically due to the high density of low-lying electronic states and the large number of low frequency vibrational modes of the underlying clusters. This is not unexpected, considering the many d electrons and the possible multiple spin states, as well as the large sizes of the anions.

However, what is the nature of the sharp peaks at the high binding energy side for the smaller dianions in Figs. 4 and 5? That these peaks appeared at the same kinetic energies regardless of the photon energies suggested that they do not reflect the normal photodetachment transitions and they must be due to a new electron emission channel. The various experimental observations made about these features suggested that they were probably due to electron tunnelling through the RCB, a process analogous to thermionic emission. The absorbed photon in a cluster anion can either induce the emission of an electron or be converted into the internal energy of the cluster anions, producing a "super" hot cluster anion. These "super" hot clusters, $[Ru_6C(CO)_n^{2-}]^*$ and $[Ru_6(CO)_n^{2-}]^*$, can either dissociate to give a CO neutral fragment ($CO + Ru_6C(CO)_{n-1}^{2-}/Ru_6(CO)_{n-1}^{2-}$) or boil off one electron [thermionic emission, $e + Ru_6C(CO)_n^-/Ru_6(CO)_n^-$] with slow kinetic energies. Because the smaller complexes have electron binding energies close to zero, the thermionic emission would be expected to be the dominating process. These thermally emitted electrons would have to tunnel through the RCB with certain kinetic energies and thus would be independent of the photon energies. The hot cluster complexes from the CID processes would also favor the thermionic emissions. Thermionic emission is commonly observed in photodetachment of cluster anions as low binding energy tails (near zero eV electrons).[33] But this is the first observation of such processes in doubly charged anions, where the RCB dominates and the thermionic electrons have to occur at certain kinetic energies.

V. CONCLUSIONS

We report a combined EDESI–MS and PES study of three polynuclear transition metal carbonyl clusters,

$Ru_3Co(CO)_n^-$, $Ru_6C(CO)_n^{2-}$, and $Ru_6(CO)_n^{2-}$. The EDESI–MS map of the monoanion $Ru_3Co(CO)_{13}^-$ showed a simple pattern of CO loss from the parent cluster to the metal core as the cone voltage is increased. PES spectra of $Ru_3Co(CO)_n^-$ ($n=0–13$) were obtained, revealing a high density of electronic states for all the clusters. The electron binding energies of the $Ru_3Co(CO)_n^-$ clusters were almost constant from $n=13$ to 4, but decrease sharply from $n=4$ to 0. The EDESI–MS maps of the dianionic species were more interesting, showing CO losses from the parents until $n=9$ with increasing cone voltage. For $n<9$ only monoanions were observed. The PES spectra of the dianion complexes revealed their electronic stability and indicated that the electron binding energies of both dianion series decrease with loss of CO and approach to 0 eV at $n=9$, in precise agreement with the EDESI–MS observations. The high density of electronic states again only yielded broad PES spectra for all the dianionic complexes. The electron binding energies of $Ru_6C(CO)_n^{2-}$ were observed to be consistently larger than that of $Ru_6(CO)_n^{2-}$.

ACKNOWLEDGMENTS

[1] F. A. Cotton, G. Wilkinson, C. A. Murillo, and M. Bochmann, *Advanced Inorganic Chemistry*, 6th ed. (Wiley, New York, 1999).

[2] E. L. Muetterties and J. Stein, Chem. Rev. **79**, 479 (1979); S. H. Langer, *ibid.* **81**, 109 (1981); J. A. M. Simões and J. L. Beauchamp, *ibid.* **90**, 629 (1990).

[3] T. Rhodin and C. Bruker, *Characterization of Metal and Polymer Surface* (Academic, New York, 1977), Vol. I, M. Kiskinova, in *New Trends in CO Activation*, edited by L. Guczi (Elsevier, New York, 1991).

[4] M. J. S. Dewar, Bull. Soc. Chim. Fr. **18**, C79 (1951); J. Chatt and L. A. Duncanson, J. Chem. Soc. **1953**, 2929.

[5] C. W. Bauschlicher and P. S. Bagus, J. Chem. Phys. **81**, 5889 (1984); C. W. Bauschlicher, S. R. Langhoff, and L. A. Barnes, Chem. Rev. **129**, 431 (1989).

[6] E. R. Davidson, K. L. Kunze, F. B. C. Machado, and S. J. Chakravorty, Acc. Chem. Res. **26**, 628 (1993); A. Veillaro, Chem. Rev. **91**, 743 (1991).

[7] A. W. Ehlers, S. Dapprich, S. F. Vyboishchikov, and G. Frenking, Organometallics **15**, 105 (1996); A. Diefenbach, M. Bickelhaupt, and G. Frenking, J. Am. Chem. Soc. **122**, 6449 (2000).

[8] M. Zhou, L. Andrews, and C. W. Bauschlicher, Chem. Rev. **101**, 1931 (2001); L. S. Sunderlin, D. Wang, and R. R. Squires, J. Am. Chem. Soc. **114**, 2788 (1992); F. Qi, X. Yang, S. Yang, F. Liu, L. Sheng, H. Gao, Y. Zhang, and S. Yu, J. Chem. Phys. **106**, 9474 (1997).

[9] R. H. Schultz, K. C. Crellin, and P. B. Armentrout, J. Am. Chem. Soc. **113**, 8590 (1991); F. A. Khan, D. E. Clemmer, R. H. Schultz, and P. B. Armen-

trout, J. Phys. Chem. **97**, 7978 (1993); F. Meyer and P. B. Armentrout, Mol. Phys. **88**, 187 (1996); X. Ren, P. A. Hintz, and K. M. Ervin, J. Chem. Phys. **99**, 3575 (1993); A. Grushow and K. M. Ervin, *ibid.* **106**, 9580 (1997).

[10] P. W. Villalta and D. G. Leopold, J. Chem. Phys. **98**, 7730 (1993); A. A. Bengali, S. M. Casey, C.-L. Cheng, J. P. Dick, T. Fenn, P. W. Villalta, and D. G. Leopold, J. Am. Chem. Soc. **114**, 5257 (1992); A. E. Stevens, C. S. Feigerle, and W. C. Lineberger, *ibid.* **104**, 5026 (1982); S. A. Klopcic, V. D. Moravec, and C. C. Jarrold, J. Chem. Phys. **110**, 8986 (1999); G. S. Icking-Konert, H. Handschuh, G. Gantefor, and W. Eberhardt, Phys. Rev. Lett. **76**, 1047 (1996); Int. J. Mass Spectrom. Ion Processes **159**, 81 (1996).

[11] H. Jacobsen and T. Ziegler, J. Am. Chem. Soc. **118**, 4631 (1996); T. A. Barckholtz and B. E. Bursten, *ibid.* **120**, 1926 (1998).

[12] G. Critchley, P. J. Dyson, B. F. G. Johnson, J. S. McIndoe, R. K. O'Reilly, and P. R. R. Langridge-Smith, Organometallics **18**, 4090 (1999); R. J. H. Clark, P. J. Dyson, D. G. Humphrey, and B. F. G. Johnson, Polyhedron **17**, 2985 (1998); D. H. Farrar, B. F. G. Johnson, J. Lewis, N. Nicholls, P. R. Raithby, and M. J. Rosales, J. Chem. Soc. Chem. Commun. **1981**, 273.

[13] P. F. Jackson, B. F. G. Johnson, J. Lewis, and P. R. Raithby, J. Chem. Soc. Chem. Commun. **1980**, 60; C. R. Eady, B. F. G. Johnson, and J. Lewis, *ibid.* **1976**, 302; D. H. Farrar, B. F. G. Johnson, J. Lewis, P. R. Raithby, and M. J. Rosales, J. Chem. Soc. Dalton Trans. **1982**, 2051.

[14] P. J. Dyson, N. Feeder, B. F. G. Johnson, J. S. McIndoe, and P. R. R. Langridge-Smith, J. Chem. Soc. Dalton Trans. **2000**, 1813; P. J. Dyson, A. K. Hearley, B. F. G. Johnson, J. S. McIndoe, and P. R. R. Langridge-Smith, Organometallics **20**, 3970 (2001); P. J. Dyson, A. K. Hearley, B. F. G. Johnson, J. S. McIndoe, and P. R. R. Langridge-Smith, J. Cluster Sci. **12**, 273 (2001).

[15] P. J. Dyson, B. F. G. Johnson, J. S. McIndoe, and P. R. R. Langridge-Smith, Rapid Commun. Mass Spectrom. **14**, 311 (2000).

[16] P. J. Dyson, A. K. Hearley, B. F. G. Johnson, J. S. McIndoe, P. R. R. Langridge-Smith, and C. Whyte, Rapid Commun. Mass Spectrom. **15**, 895 (2001).

[17] L. S. Wang, C. F. Ding, X. B. Wang, and S. E. Barlow, Rev. Sci. Instrum. **70**, 1957 (1999).

[18] L. S. Wang and X. B. Wang, J. Phys. Chem. A **104**, 1978 (2000).

[19] X. B. Wang and L. S. Wang, J. Phys. Chem. A **104**, 4429 (2000); J. Am. Chem. Soc. **122**, 2339 (2000); **122**, 2096 (2000); J. Chem. Phys. **111**, 4497 (1999).

[20] X. B. Wang, L. S. Wang, R. Brown, P. Schwerdtfeger, D. Schroder, and H. Schwarz, J. Chem. Phys. **114**, 7388 (2001); X. B. Wang and L. S. Wang, *ibid.* **112**, 6959 (2000); G. L. Gutsev, B. K. Rao, P. Jena, X. B. Wang, and L. S. Wang, Chem. Phys. Lett. **312**, 598 (1999); X. B. Wang, C. F. Ding, L. S. Wang, A. I. Boldyrev, and J. Simons, J. Chem. Phys. **110**, 4763 (1999).

[21] X. B. Wang and L. S. Wang, Phys. Rev. Lett. **83**, 3402 (1999).

[22] X. B. Wang and L. S. Wang, Nature (London) **400**, 245 (1999).

[23] G. L. Geoffroy, J. R. Fox, E. Burkhardt, H. C. Foley, A. D. Harley, and R. Rosen, Inorg. Synth. **21**, 57 (1982).

[24] C. T. Hayward and J. R. Shapley, Inorg. Chem. **21**, 3816 (1983).

[25] P. J. Bailey, M. A. Beswick, J. Lewis, P. R. Raithby, and M. C. Ramirez de Arelano, J. Organomet. Chem. **459**, 293 (1993).

[26] M. K. Scheller, R. N. Compton, and L. S. Cederbaum, Science **270**, 116 (1995).

[27] A. I. Boldyrev, M. Gutowski, and J. Simons, Acc. Chem. Res. **29**, 497 (1996).

[28] X. B. Wang, C. F. Ding, J. B. Nicholas, D. A. Dixon, and L. S. Wang, J. Phys. Chem. A **103**, 3423 (1999).

[29] X. B. Wang, J. B. Nicholas, and L. S. Wang, J. Chem. Phys. **113**, 10837 (2000).

[30] X. Li and L. S. Wang (unpublished).

[31] L. S. Wang and X. Li, in *International Symposium on Clusters and Nanostructure Interfaces* (Oct. 25–28, 1999, Richmond, VA), edited by P. Jena, S. N. Khanna, and B. K. Rao (World Scientific, New Jersey, 2000).

[32] J. Akola, M. Manninen, H. Hakkinen, U. Landman, X. Li, and L. S. Wang, Phys. Rev. B **60**, 11297 (1999).

[33] L. S. Wang, J. Conceicao, C. Jin, and R. E. Smalley, Chem. Phys. Lett. **182**, 5 (1991); G. Gantefor, W. Eberhardt, H. Weidele, D. Kreisle, and E. Recknagel, Phys. Rev. Lett. **77**, 4524 (1996).